THE POTENTIAL DISTRIBUTION ON THE BODY SURFACE CAUSED BY A HEART VECTOR

CALCULATIONS ON SOME SIMPLE MODELS

H. C. BURGER, D.SC.,* H. A. TOLHOEK, D.SC.,** AND F. G. BACKBIER, M.S.**

UTRECHT, NETHERLANDS

I. INTRODUCTION

THE electrical action of the heart may be described to a certain approximation by one single vector, the heart vector. The classical equilateral triangle of Einthoven and associates[1] provided a means of finding this vector from the extremity leads. The true relation between the heart vector and leads, however, is a more complicated one. As has been pointed out previously,[2,4] the potential difference V_{PQ} between two electrodes P and Q is a linear function of the components X, Y, Z of the heart vector

$$V_{PQ} = aX + bY + cZ \ . \qquad (1)$$

The coefficients a, b, c remain constant during the heart beat and depend on the shape and conductive properties of the trunk. They can be determined on a phantom or on dead human bodies. But apart from this experimental method, it may be useful to treat the problem mathematically. This can only be done, however, by making some very simplifying assumptions. If the trunk is treated as a homogeneous sphere with the heart vector (dipole) acting in its center, the solution can be readily given and is a three dimensional generalization of the Einthoven triangle. If the position of the heart is not central, however, a more complicated mathematical treatment is required. Wilson and Bayley[5] have treated this case, and they have given explicit formulas for the potential distribution.

The shape of the human trunk, however, is more like a cylinder than like a sphere. It was thought desirable, therefore, to calculate the potential distribution on a cylinder generated by a dipole. To avoid too complicated calculations, the cylinder is chosen circular, and the dipole is placed on its axis. Furthermore, it is assumed to be homogeneous, since a theoretical treatment of the conduction in a heterogeneous cylinder seems to be hardly possible. The shape of the cylinder is seen from Fig. 1. The ratio of the radius to the height, as well as the position of the dipole (heart), can be chosen arbitrarily. However, since a numerical calculation is required and the result cannot be given in explicit formulas, we had to decide upon these ratios. We have chosen a cylinder with radius R and the upper and lower boundary plane at $z = -1.5$ and $z = 2.2$ R, respectively. (The position of the dipole, the heart, is chosen as the origin.)

The closed cylinder may be a fairly good approximation of the actual case. However, the body is flattened and the heart is eccentrically placed. To give a

Received for publication Feb. 16, 1954.

*Department of Medical Physics, Physical Laboratory, University, Utrecht, Netherlands

**Institute for Theoretical Physics, University, Utrecht, Netherlands.

qualitative discussion of differences in the shape of the model on the potential distribution, we also discuss the potential distribution on the open (infinite) cylinder, and on two parallel planes, caused by a dipole.

II. GEOMETRICAL REPRESENTATION BY MEANS OF AN IMAGE SURFACE

In a previous paper[4] one of us, in collaboration with J. B. van Milaan, developed a geometrical representation of the relation between the heart vector and leads, the boundary of the trunk, and its heterogeneity being quite arbitrary. This representation can be deduced from Equation (1), in which X, Y, Z are components of a vector, the heart vector, and V_{PQ} is a potential difference and therefore a scalar quantity. It can be shown from this that the coefficients $\overrightarrow{a, b, c}$ must have the character of vector components. So there is a vector a, b, c. The relation, Equation (1), can be interpreted geometrically: the potential difference V_{PQ} equals the projection of the heart vector $\overrightarrow{X, Y, Z}$ on the vector $\overrightarrow{a, b, c}$ times the length of the latter. It is the so-called scalar product of both vectors.

We take for Q a fixed point on the body surface. Then to each point P on this surface a vector $\overrightarrow{a, b, c}$ corresponds according to Equation (1). This vector may be drawn from a fixed origin. The terminus P′ of this vector can be considered as an image of the point P. To each point P of the body belongs a point P′ in the image space. The locus of all points P′ is the image of the real body surface. The potential distribution on the real body surface can be deduced from the image surface, if the correspondence of the points P and P′ everywhere on the surface is known, and so for any arbitrary direction of the heart vector. To find the potential difference of two points P and Q we have only to find the corresponding points P′ and Q′ on the image surface and to project the heart vector on the line P′Q′. The product of the projection and the length of P′Q′ is equal to the potential difference between P and Q.

In the following sections we shall calculate the image surface for some mathematically single cases (body surface is an open cylinder, a closed cylinder, and two parallel planes, respectively). By some examples we shall show how the image surface can be used.

III. THE POTENTIAL DISTRIBUTION ON AN OPEN (INFINITE) CYLINDER

The dipole can be decomposed into two components, one along the axis of the cylinder and the other perpendicular to it. We calculate the field separately for both cases and calculate the field in an open infinite cylinder (without boundaries at the top and at the bottom).

We shall use cylindrical coordinates r, ϑ, z; their relation to the Cartesian coordinates, x, y, z is shown in Fig. 1. Inside the cylinder the potential φ (r, ϑ, z) is a function of the cylindrical coordinates r, ϑ, z (or of the rectangular coordinates x, y, z). This function obeys a differential equation, expressing that there is no electric charge inside the cylinder. In rectangular coordinates this equation has the simple form:

$$\frac{\partial^2\varphi}{\partial x^2} + \frac{\partial^2\varphi}{\partial y^2} + \frac{\partial^2\varphi}{\partial z^2} = 0, \text{ or abbreviated } \Delta\varphi = 0.$$

The way in which this is expressed in the cylindrical coordinates r, ϑ, z can be found in Appendix I.

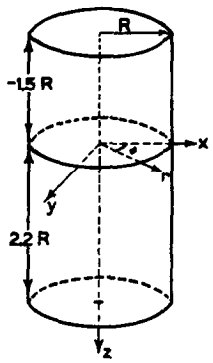

Fig. 1.

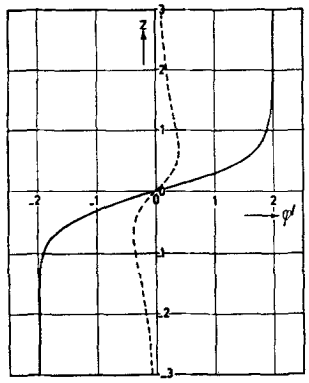

Fig. 2.

Fig. 1.—Shape of the cylinder for which the potential distribution is calculated. The position of the dipole (the heart) is taken as the origin of the coordinate system. The relations between the Cartesian coordinates (*x*, *y*, *z*) and the cylindrical coordinates (*r*, ϑ, *z*) are also shown.

Fig. 2.—The potential φ''(R, z), caused by a dipole parallel to the axis of the infinite cylinder on its surface, as a function of z. The dotted line shows the potential at the same places, if the entire space is filled with the conducting medium.

At the origin, where the dipole is assumed to be acting, φ must become infinite and no longer satisfies $\Delta\varphi = 0$. We require that φ obey the following expression near the origin:

$$\varphi\left(\frac{\rightarrow}{\rho}\right) = \frac{\rightarrow}{p}\cos\gamma/\rho^2 \tag{2}$$

($\vec{p}$ is the dipole moment and $\vec{\rho}$ the radius vector, γ is the angle between the vectors $\vec{p}$ and $\vec{\rho}$). At the surface of the "trunk," i.e., at the cylindrical surface, the normal component of the current density is zero, thus $\frac{\partial\varphi}{\partial n} = 0$ (n being the direction normal to the surface).

In Appendix I the general mathematical treatment is given. In Appendix II the calculations are carried out for a dipole parallel to the axis of an infinite cylinder. The potential does not depend on ϑ since rotational symmetry exists and we can write φ'' (r,z). The results for the surface of the cylinder and for a dipole of unit moment are given in Fig. 2. (For comparison, we have also drawn the potential which would be caused by the same dipole in infinite space at the same places.)

In Appendix III the formulas are given for the potential of a unit dipole perpendicular to the axis of an infinite cylinder. If the dipole is directed along the x-axis, we shall denote the potential by φ^*(r, ϑ, z). It appears to be the product of a function F^*(r,z) of r and z only and cos ϑ, so on the surface of the cylinder:

$$\varphi^*(r, \vartheta, z) = F^*(z)\cos\vartheta\ . \tag{3}$$

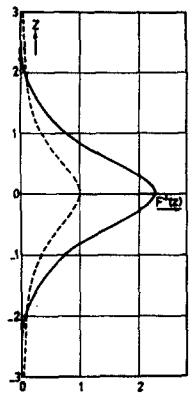

Fig. 3.—The potential $F^{\wedge}(z)$, caused by a dipole in the x-direction perpendicular to the axis of the infinite cylinder, on the generating line x = 0, y = 1 of its surface, as a function of z. The dotted line shows the potential at the same places if the entire space is filled with the conducting medium.

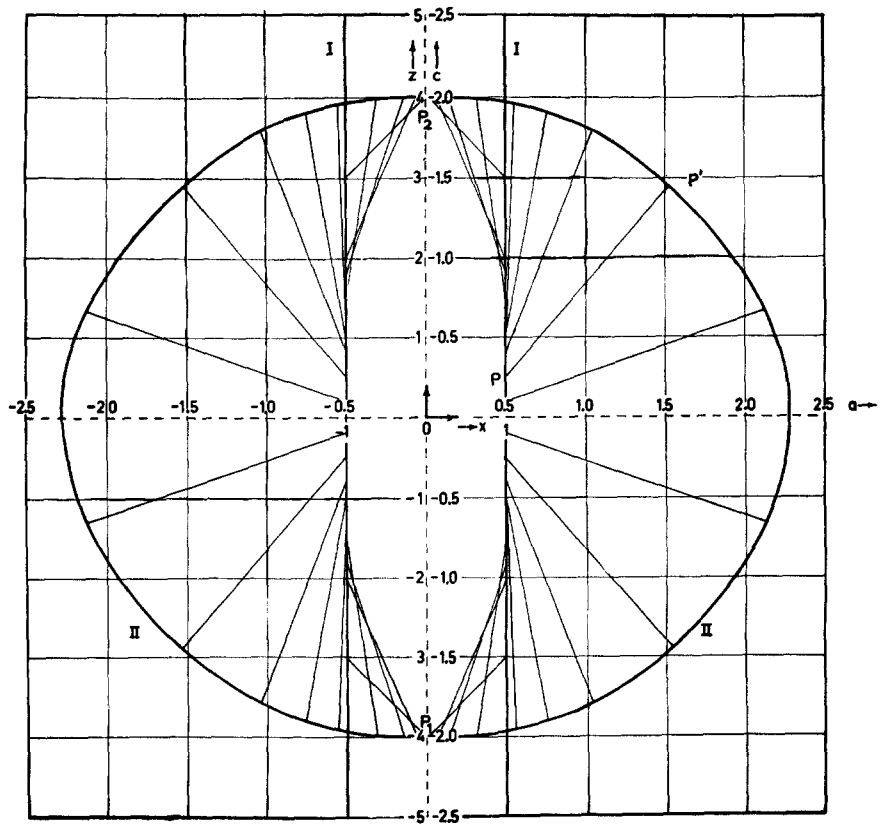

Fig. 4.—The image surface of an infinite cylinder. The correspondence between a point P of the cylinder and P' of the image surface is indicated by a straight line. *I*, Intersection of the cylinder with the x-z plane. *II*, Intersection of the image surface with the a-c plane.

The function $F^{*}(z)$ is represented in Fig. 3 (again the potential of the same dipole in infinite space is drawn for comparison).

We now give the results for the potential distribution by means of an image surface. If X, Y, Z are the components of the heart vector, the potential φ can be composed of contributions from each of these components. Z, parallel to the axis of the cylinder gives:

$$\varphi_z = Z\varphi''(r, z) .$$

X and Y, perpendicular to the axis of the cylinder give:

$$\begin{aligned} \varphi_x &= X\varphi^{*}(r, \vartheta, z) = XF^{*}(z)\cos\vartheta \\ \varphi_y &= YF^{*}(z)\sin\vartheta . \end{aligned}$$

So the total value of the potential is:

$$\varphi = \varphi_x + \varphi_y + \varphi_z = XF^{*}(z)\cos\vartheta + YF^{*}(z)\sin\vartheta + Z\varphi''(r, z) .$$

Comparing with Equation (1) we conclude that the coefficients a, b, c for the surface of the cylinder are given by

$$c(R, z) = \varphi''(R, z) \quad (4)$$
$$a(R, \vartheta, z) = F^{*}(z)\cos\vartheta \quad (5)$$
$$b(R, \vartheta, z) = F^{*}(z)\sin\vartheta . \quad (6)$$

The directions of the a, b, c axes are parallel to those of the X, Y, Z axes. The origin of the a, b, c space (image space) may be chosen at will. The reference potential, with which the potential of a point P is compared, is the mean value of the potential at $z = +\infty$ and $z = -\infty$.

It follows from Equations (5) and (6) that the image surface has the c-axis as the axis of rotational symmetry. In Fig. 4 we have drawn the intersection of the infinite cylinder with the x-z plane and, in the same figure, the intersection of its image surface with the a-c plane. The correspondence between a point P of the cylinder surface and the point P′ of the image surface is indicated by a straight line joining P and P′.

The parts of the cylinder that are a great distance from the dipole have their image approximately in two points of the image surface, namely, P_1 and P_2.

IV. THE POTENTIAL DISTRIBUTION ON A CLOSED (FINITE) CYLINDER

In Appendix IV we have given the method of calculation for the potential distribution on the surface of a cylinder bounded by two planes $z = -1.5$ R and $z = 2.2$ R. This can be done starting from the results of Appendices II and III using the method of electrical images. The results are represented in Figs. 5 and 6 for a dipole parallel to the axis, and in Figs. 7 and 8 for a dipole perpendicular to the axis of the cylinder. Notations are analogous to those for the infinite cylinder, but the index b denotes that we have a closed cylinder. We have, for example:

$$\varphi_b^{*}(r, \vartheta, z) = F_b^{*}\cos\vartheta . \quad (7)$$

It should be noted that the planes $z = -1.5$ R and $z = 2.2$ R are now part of the surface of the body while they are situated in the interior of the body for

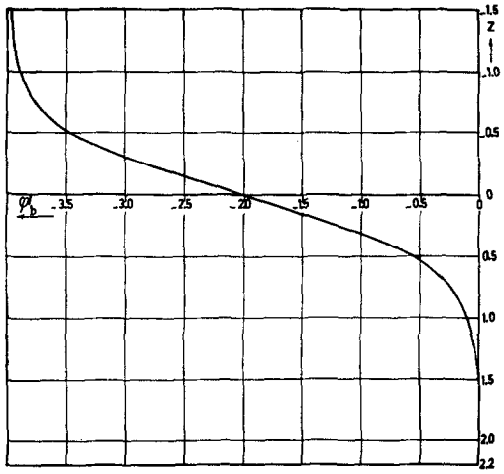

Fig. 5.

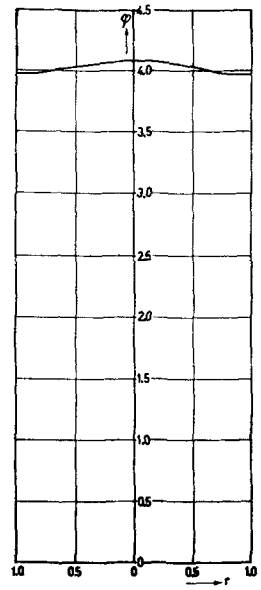

Fig. 6.

Fig. 5.—The potential $\varphi_b''(R, z)$, caused by a dipole parallel to the axis of the finite cylinder on its surface, as a function of z.

Fig. 6.—The potential, caused by a dipole parallel to the axis of the finite cylinder on the boundary plane $z = -1.5$ R, as a function of r.

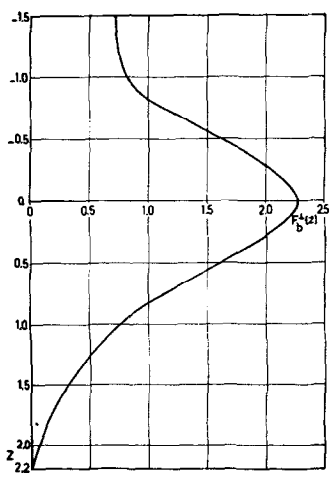

Fig. 7.

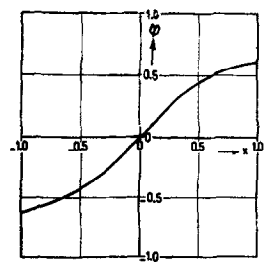

Fig. 8.

Fig. 7.—The potential $F_b^+(z)$, caused by a dipole in the x-direction on the generating line $x = 0$, $y = 1$ of the surface of the finite cylinder, as a function of z.

Fig. 8.—The potential, caused by a dipole in the x-direction on the boundary plane $z = -1.5$ R, as a function of x (on the line $y = 0$, $z = -1.5$ R).

the infinite cylinder. We see from the figures that the differences with the infinite cylinder are not very great. (Compare Fig. 5 with Fig. 2 and Fig. 7 with Fig. 3.)

In Fig. 9 and Fig. 10, we have given diagrams of the equipotential lines on the surface of the cylinder for the parallel and the perpendicular dipoles, respectively.

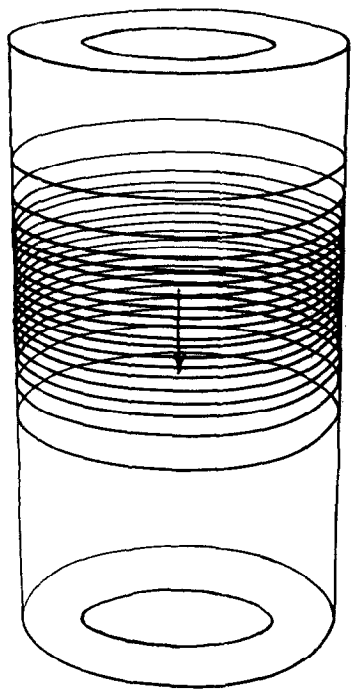

Flg. 9.

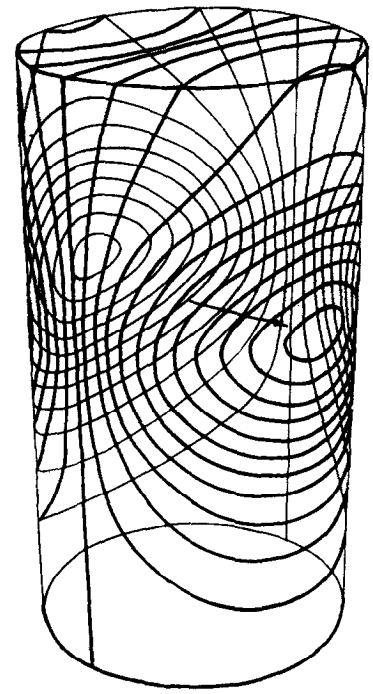

Fig. 10.

Fig. 9.—Equipotential lines on the cylinder surface for a dipole parallel to the axis. Two succeeding equipotential lines have a potential difference of 0.2.

Fig. 10.—Equipotential lines on the cylinder surface for a dipole perpendicular to the axis. Two succeeding equipotential lines have a potential difference of 0.2.

We can again represent the potential distributions by means of an image surface. The center of the lower boundary plane ($z = 2.2$ R) will be taken as reference point Q, where the potential of the finite cylinder is taken to be zero. As in Section III, the values of a, b, and c for the surface of the cylinder follow from the potential distributions caused by dipoles in the x, y and z directions. Likewise, the image surface has rotational symmetry about the c-axis. In Fig. 11, we have drawn the intersection of the cylinder with the x-z plane and in the same figure, the intersection of its image surface with the a-c plane. The correspondence between points of body and image surface is indicated in the same way as in Fig. 4.

The image surface does not differ very much from a sphere. It is remarkable that no visible edges of the image surface correspond to the edges of the cylinder. The lower end of the cylinder (especially the lower boundary plane) has its image nearly in one point—the lowest point of the image surface. This means that this part of the cylinder shows hardly any potential differences.

V. THE POTENTIAL DISTRIBUTION ON TWO PARALLEL PLANES

The field of a dipole (at the origin of a Cartesian coordinate system) between two parallel planes $y = A$ and $y = -3$ A can be calculated with the method of electrical images discussed in Appendix IV. We have represented the results by means of an image surface in the same way as in Sections III and IV (Fig. 12). The two parallel planes can be considered as a model of an extremely flattened trunk. The heart is placed at one-fourth of the distance between the front plane and the back plane. It is seen that this results in a large asymmetry of the image surface. The image surface has the b-axis as the axis of rotational symmetry.

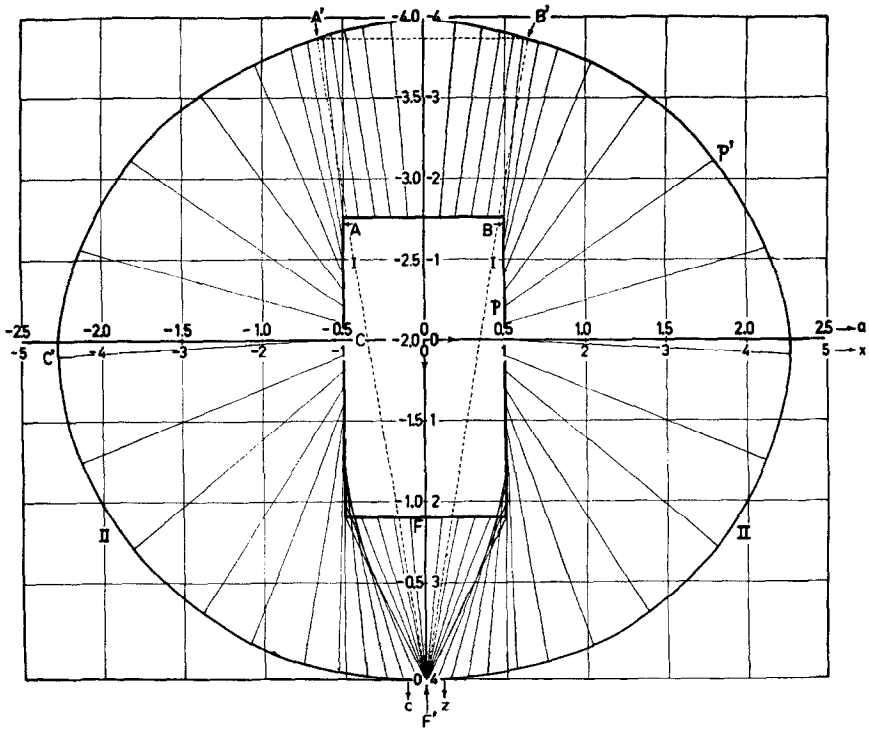

Fig. 11.—The image surface of the finite cylinder shown in Fig. 1. *I*, Intersection of the cylinder with the x-z plane. *II*, Intersection of the image with the a-c plane. The correspondence between a point *P* of the cylinder and *P'* of the image surface is indicated by a straight line.

VI. EXAMPLES OF THE USE OF THE IMAGE SURFACE

With the aid of the image surface, several problems can be numerically solved. Its use is analogous to that of the Einthoven triangle. The potential difference between two points of the body surface is equal to the projection of the heart vector on the line joining their *images* (not the points themselves) *multiplied by the length of this image-line.* In the following paragraphs, a few examples are given for the finite, closed cylinder (Fig. 11).

A.—It is easy to draw in Fig. 11 the triangle analogous to that of Einthoven. The arms correspond to the points A and B in the symmetry plane, about 0.1 R below the upper boundary plane of the cylinder, the (left) foot corresponds to the center F of the lower boundary plane. It appears that the triangle A'B'F' is not equilateral but very narrow. As a consequence of this,

the potential difference between A and B (Lead I) is relatively small, for it is equal to the product of the projection of the heart vector on A′B′ and the length of A′B′. This length is much smaller than A′F′ = B′F′. Conversely, if the leads are given it is concluded from the narrow triangle that the horizontal component of the heart vector is large.

The analogue of the equilateral tetrahedron can also be constructed, accepting that the back electrode is situated just behind the dipole (heart). Although in Fig. 11 only a plane drawing is given, the rotational symmetry of the cylinder permits the position of the image of the back electrode to be found. To this end, the points C and C′ have to be rotated 90 degrees about the symmetry axis till they lie behind the dipole. C′ must then be combined with the apices of the triangle A′B′F′, mentioned previously.

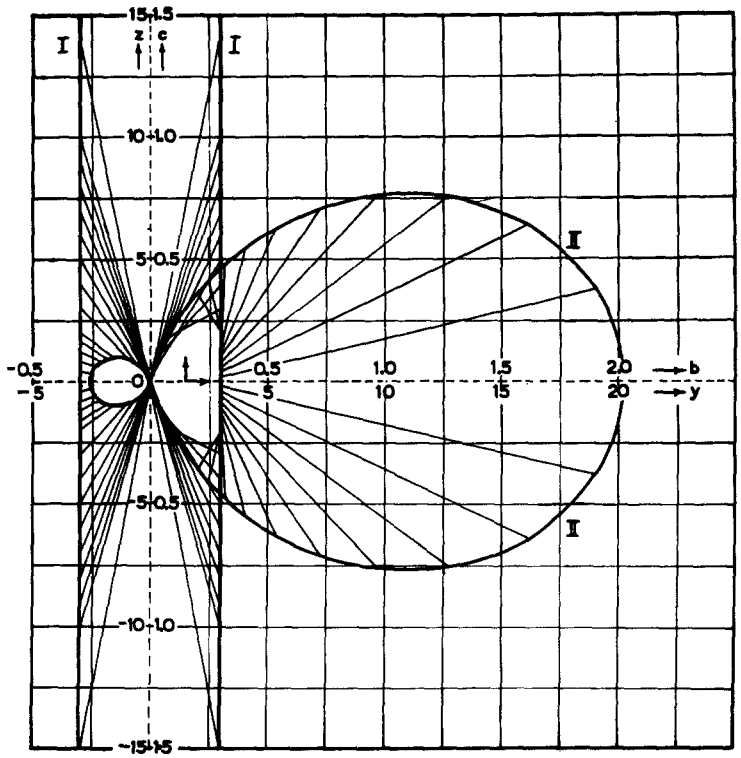

Fig. 12.—The image surface of two parallel planes with an eccentric dipole. *I*, Intersection of the two planes with the y-z plane. *II*, Intersection of the image surface with the b-c plane. The planes are placed at y = ±3; the dipole at y = 1.5, z = 0.

B.—If the heart vector is perpendicular to the axis of the cylindrical trunk, its projection on a vertical generating line is zero. The conclusion that the potential difference between the ends A and B of such a line (Fig. 13) be zero should be incorrect. The projection of the heart vector has to take place on the line A′B′ in the image space, and it appears that the potential difference between A and B is 50 per cent of that between the diametral points A and a of the top surface.

C.—We can calculate the potential difference between two diametral points p and P (Fig. 13) of the cylinder at the same height as a function of their height, the heart vector being horizontal. This potential difference is not independent of this height, as is the projection of the heart vector (dipole) on the line joining the diametral points. Its variation ranges from 27 per cent for aA to 0 per cent for bB of its maximum value, which is attained nearly at the same height as the heart. This potential difference is not inversely proportional to the square of the distance of the electrodes to the heart, nor to the square of the distance of the line joining them to the heart. This may be easily verified by the reader.

D.—If it is assumed that the projection of the heart vector on a line joining two electrodes is a measure of the potential difference between these electrodes, an error is made that depends on various circumstances. The following numerical example gives an idea of the error that can be made.

A heart vector making an angle of 45 degrees with the symmetry axis of the cylinder (pointing downward) gives potential differences between the "arms" (see *A*) and between an arm and the feet of 130 and 330 in an arbitrary measure. This can be deduced from Fig. 11. If we do not remember that these values have to be deduced, using the image surface in the correct manner, we may be inclined to suppose that the ratio of the aforementioned values 130/330 is the ratio of the projection of the heart vector on a horizontal and a vertical line, respectively. In this way the angle of the vector with the vertical line is computed to be 21 degrees instead of 45 degrees.

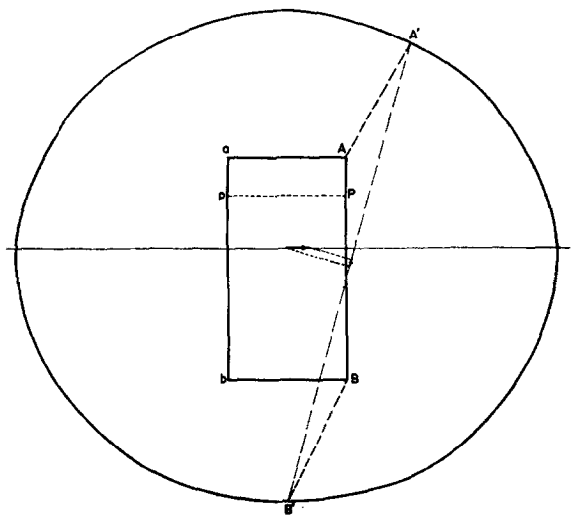

Fig. 13.—Illustration of the use of the image surface for a finite (closed) cylinder.

VII. DISCUSSION

Our models differ from the human body in many respects. Their shape and the position of the heart are not in accordance with the facts and a serious disadvantage is that the electrical heterogeneity of the human body is not taken into account. A much better approximation is the model we used previously.[3] The models referred to in the present paper, however, have an advantage in that the calculations give the image surface in a simple mathematical form, in such a way that it can be evaluated numerically.

The Einthoven triangle and its spatial generalization, the regular tetrahedron,[7] are based on the assumption of a homogeneous body, either extending infinitely or spherical. They are just as correct models as any other, though very imperfect ones. If a geometric shape has to be chosen, the closed cylinder is a much better approximation to the body shape than the sphere.

Our mathematical considerations allow us to draw some general conclusions as to the relation of the shape of the image surface to the shape of the body surface. A protruding part of the body surface, such as an arm or a leg, nearly corresponds to a single point in the image space. This is shown in the case of the infinite cylinder, the infinitely long ends of which are represented as one point (P_1 and P_2) of the image surface (Fig. 4). In the case of the extremity

leads it is therefore arbitrary *where* the electrode is placed on arm or leg. All points of the arm (or leg) are in the image space identical, as if shriveled up to one point.

An inward displacement of the body surface causes an outward displacement of the image surface at the same side. This is seen when the open and the closed cylinders are compared. Analogous to an inward displacement of the body surface is a displacement of the heart towards it. The outward displacement of the image surface caused by it is shown by Fig. 12 for the parallel planes, where this surface has a protruding part at the side nearest the heart. This gives an idea of the deformation of the image surface to be expected if the heart were situated eccentrically in a cylinder. The same must be true in the human body where the heart is situated near the frontal thoracic wall. The image surface of the human body has a protruding part at the frontal side. Consequently, there is a large potential difference between a precordial electrode and an indifferent electrode anywhere on the body surface according to the rules given in the preceding pages. The nearer the "heart," that is the dipole, is situated to the body surface the more protrudes the corresponding part of the image surface. The shape of the latter will, therefore, depend for the greater part on the position of the dipole. This position may vary considerably inside the heart and as its dimensions cannot be neglected, the image surface differs appreciably for different parts of the heart. This is especially true for the protruding part and therefore for precordial electrodes. It is to be expected that for these cases the description of the phenomena with a single image surface will not be a sufficient approximation.

It should be possible to calculate the image surface in a simple case, the heart lying near the body surface by proceeding from the case of the parallel planes. With two other pairs of planes the space might be bounded such that a rectangular prism is formed in which the heart is situated close to one of the planes. This requires, however, rather extensive calculations, which we have not carried out.

SUMMARY

A mathematical treatment of the dipole field in a bounded space is given for a few simple cases. The potential at the surface is calculated for an open and for a closed cylinder with the dipole on its axis, and for an infinite layer bounded by two parallel planes, the dipole being situated nearer to one plane than to the other. The medium is assumed to be homogeneous. The image surface introduced in a previous paper is calculated and represented in Figs. 4, 11, 12, and 13. A few examples illustrate the use of this surface.

APPENDIX I. MATHEMATICAL FORMULATION OF THE PROBLEM: METHOD OF SOLUTION

We now give the method used to calculate the potential φ in an infinite cylinder, discussed in Section II. φ must satisfy the potential equation which we write in cylindrical coordinates

$$\frac{1}{r}\frac{\partial}{\partial r}\left(r\frac{\partial \varphi}{\partial r}\right)+\frac{1}{r^2}\frac{\partial^2 \varphi}{\partial r^2}+\frac{\partial^2 \varphi}{\partial z^2}=0\,. \tag{A 1}$$

The boundary condition for a cylinder of radius R reads

$$\left(\frac{\partial \varphi}{\partial r}\right)_{r=R} = 0 \quad . \tag{A 2}$$

In the neighborhood of the origin φ must obey the expression

$$\varphi = \vec{p} \cdot \vec{\rho}/\rho^3 = p \cos \gamma/\rho^2, \vec{\rho} \simeq 0 \tag{A 3}$$

($\vec{\rho}$ is the radius vector from the origin; $\rho = \sqrt{r^2 + z^2}$.) Using the standard method of separation of the variables r, ϑ, z, in (A 1), we obtain a potential which satisfies (A 1) everywhere. This potential can be expressed in the following form (Fourier series and Fourier integral)

$$\varphi(r, \vartheta, z) = \sum_{n=-\infty}^{\infty} \exp(in\vartheta) \int_{-\infty}^{\infty} A_{n,\alpha} I_n(\alpha r) \exp(i\alpha z)\, d\alpha \tag{A 4}$$

$A_{n,\alpha}$ depends only on n and α. $I_n(\alpha r)$ is a Bessel function of order n (see notation of Ref. 6, p. 25 ff.). We desire a solution (A 4) which satisfies the boundary condition

$$\left(\frac{\partial \varphi}{\partial r}\right)_{r=R} = g(\vartheta, z) \ . \tag{A 5}$$

Assuming $g(\vartheta, z)$ can be expanded in a Fourier series

$$g(\vartheta, z) = \sum_{n=-\infty}^{\infty} \int_{-\infty}^{\infty} B_{n,\alpha} \exp(in\vartheta) \exp(i\alpha z)\, d\alpha \tag{A 6}$$

then, from (A 4), (A 5) and (A 6), the value of $A_{n,\alpha}$ follows

$$A_{n,\alpha} = B_{n,\alpha}/\alpha\, I_n^1(\alpha) \ . \tag{A 7}$$

This value of $A_{n,\alpha}$ substituted in (A 4) gives a potential $\varphi(r, \vartheta, z)$ which satisfies the potential equation (A 1) everywhere within the cylinder and which satisfies the boundary condition (A 5). However, we want to calculate a potential φ which satisfies (A 1) everywhere within the cylinder except in the origin, where it must have the singularity (A 3).

Furthermore, the boundary condition (A 2) must be satisfied. This problem can be reduced to the preceding one by putting

$$\varphi = \varphi_0 + \varphi_1 \tag{A 8}$$

where

$$\varphi_0 = \vec{p} \cdot \vec{\rho}/\rho^3 \quad \text{(in entire space)}. \tag{A 9}$$

φ is a solution of (A 1) with the singularity (A 3) and the boundary condition (A 2). It follows that φ_1 is a solution of (A 1) without the singularity and with the boundary condition (A 5), where

$$g(\vartheta, z) = -\left[\frac{\partial}{\partial r}\left(\vec{p} \cdot \vec{\rho}/\rho^3\right)\right]_{r=R} \ . \tag{A 10}$$

Hence our problem has been reduced to finding the Fourier expansion (A 6) of this expression and calculating (A 4) with the coefficients obtained.

APPENDIX II. POTENTIAL DISTRIBUTION OF A DIPOLE PARALLEL TO THE AXIS OF AN INFINITE CYLINDER

The problem of Appendix I is specialized to the extent that the vector $\vec{p}$ of (A 9) is now a vector in the direction of the z-axis, and φ_0 can be expressed as

$$\varphi_0 = pz\,(r^2 + z^2)^{-\frac{3}{2}}. \tag{A 11}$$

According to (A 10) the function g (ϑ, z) becomes

$$g(\vartheta, z) = 3\,pRz\,(R^2 + z^2)^{-\frac{5}{2}}. \tag{A 12}$$

To obtain the Fourier expansion of g (ϑ, z) we use the formula given in Ref. 6, p. 163

$$\frac{1}{2}\,\frac{1}{(z^2 + R^2)^{\nu + \frac{1}{2}}} = \frac{1}{2\pi}\int_{-\infty}^{\infty} \exp(-i\alpha z)\left(\frac{|\alpha|}{2R}\right)^{\nu}\frac{\Gamma(\frac{1}{2})}{\Gamma(\nu + \frac{1}{2})}\,K_{\nu}(R\,|\alpha|)\,d\alpha, \tag{A 13}$$

where $\quad \mathrm{Re}\,\nu > -\frac{1}{2}$.

From (A 13) we obtain, by partial integration and the use of some appropriate formulas for the K_ν functions (see Ref. 6, p. 29)

$$3pRz\,(R^2 + z^2)^{-\frac{5}{2}} = \frac{ipR}{\pi}\int_{-\infty}^{\infty}\exp(i\alpha z)\,\frac{d}{d\alpha}\left[K_2(R|\alpha|)\alpha^2/R^2\right]d\alpha$$

$$= -\frac{ip}{\pi}\int_{-\infty}^{\infty}\exp(i\alpha z)\alpha|\alpha|K_1(R|\alpha|)\,d\alpha. \tag{A 14}$$

The coefficients $B_{n,\alpha}$ according to (A 6) that are derived from (A 14), are

$$B_{n,\alpha} = \begin{cases} -(ip/\pi)\alpha|\alpha|K_1(R|\alpha|), & \text{if } n = 0 \\ 0, & \text{if } n \neq 0. \end{cases} \tag{A 15}$$

Hence we see that the Fourier series has only a single term. From the values for $B_{n,\alpha}$ we get, according to (A 15) and (A 7), using the formula

$$I_0^1(\alpha R) = I_1(\alpha R) \qquad \text{(see Ref. 6, p. 29)},$$

$$A_{n,\alpha} = \begin{cases} -(ip|\alpha|/\pi)K_1(R|\alpha|)/I_1(R\alpha), & \text{if } n = 0 \\ 0, & \text{if } n \neq 0. \end{cases} \tag{A 16}$$

For φ_1 we obtain, after a simple transformation from (A 4)

$$\varphi_1(r, z) = (2p/\pi)\int_0^{\infty}\alpha K_1(\alpha R)[I_0(\alpha r)/I_1(\alpha R)]\sin\alpha z\,d\alpha. \tag{A 17}$$

The complete solution of our problem is given by (A 8). The value of φ_1 (r, z) was calculated numerically for a series of values of z for r = R and for a series of values of r for $z = z_0 = -1.5$ R. The results for φ (R, z) are given in Fig. 2. (The error is less than 1 per cent.) In these results we have taken p = 1. We remark that

$$\lim_{z = \infty}\varphi_1(R, z) = 2; \qquad \lim_{z = -\infty}\varphi_1(R, z) = -2 \tag{A 18}$$

This can be deduced rigorously from (A 17), but it can also be proved without any explicit calculation.

APPENDIX III. POTENTIAL DISTRIBUTION OF A DIPOLE PERPENDICULAR TO THE AXIS OF AN INFINITE CYLINDER

We take $\vec{p}$ in the direction of the x-axis. (A 9) then becomes

$$\varphi_0 = pr \cos \vartheta (r^2 + z^2)^{-\frac{3}{2}}. \tag{A 19}$$

The function g (ϑ, z) consequently has the form

$$g(\vartheta, z) = -p \cos \vartheta (R^2 + z^2)^{-\frac{5}{2}} (z^2 - 2R^2). \tag{A 20}$$

By partial integration and the use of appropriate formulas for the K_ν- functions,[6] we find the Fourier expansion of g (ϑ, z) from (A 13) and (A 14), which we give by the coefficients $B_{n,\alpha}$:

$$B_{n,\alpha} = \begin{cases} (p/2\pi)[\alpha^2 K_0(R|\alpha|) + |\alpha| K_1(R|\alpha|)/R], & \text{if } n = \pm 1 \\ 0, & \text{if } |n| \neq 1. \end{cases} \tag{A 21}$$

After some reductions (see Ref. 6, the formulas on p. 29), $A_{n,\alpha}$ becomes, according to (A 7),

$$A_{n,\alpha} = \begin{cases} \dfrac{p}{2\pi} \dfrac{\alpha^2 K_0(R|\alpha|) + |\alpha| K_1(R|\alpha|)/R}{\alpha I_0(R\alpha) - I_1(R\alpha)/R}, & \text{if } n = \pm 1 \\ 0, & \text{if } |n| \neq 1. \end{cases} \tag{A 22}$$

We obtain from (A 4), after some reductions, the expression for φ_1:

$$\varphi_1(r, \vartheta, z) = p \cos \vartheta \int_0^\infty \frac{2\alpha}{\pi} \frac{\alpha K_0(R\alpha) + K_1(R\alpha)/R}{\alpha I_0(R\alpha) - I_1(R\alpha)/R} I_1(\alpha r) \cos \alpha z \, d\alpha. \tag{A 23}$$

The integral in (A 23) was calculated for a number of values of z for r = R and for a number of values of r for $z = z_0 = -1.5$ R. The results for φ (r = R, ϑ = o, z) and φ (r, ϑ = o, z = z_0) are represented in Fig. 3. (The error is less than 1 per cent.)

APPENDIX IV. POTENTIALS OF DIPOLES IN A FINITE CYLINDER: METHOD OF ELECTRICAL IMAGES

If we have the solution of the potential problem for an infinite cylinder with a dipole $\vec{p}$ placed at the origin, we can derive the solution of the problem for a finite cylinder from it. Suppose the boundary planes are z = a and z = b (a < o < b) and that φ (r, ϑ, z) is the solution for the infinite cylinder. The solution for the finite cylinder is given by the sum (l = a + b)

$$\varphi_b(r, \vartheta, z) = \sum_{n=-\infty}^{\infty} \Big[\varphi(r, \vartheta, z - 2nl) + \varphi(r, \vartheta, 2a - z - 2nl) \Big]. \tag{A 24}$$

This series gives the sum of an infinite series of electrical images. We assume that the potential in any term is zero at a certain point of the body, for example, the center of the lower boundary plane. It can then be shown that no convergence difficulties exist. The potential (A 24) represents the potential of a series of dipoles as shown in Fig. 14. Hence, it satisfies the potentail equation in the interior of the finite cylinder and has the prescribed dipole singularity at the origin. As each of the terms in (A 24) satisfies the boundary condition $\left(\frac{\partial \varphi}{\partial r}\right)_{r=R} = 0$, it is also satisfied for the sum φ (r, ϑ, z). The series of images has now been chosen in such a way that the boundary condition $\left(\frac{\partial \varphi}{\partial z}\right)_{z=z_0} = 0$ is also satisfied for the upper and lower boundary planes.

The dipole, with its images, is a distribution of current sources symmetrical with respect to both the $z = a$ and the $z = b$ planes, from which the boundary condition follows. For the actual calculation of the potential in the finite cylinder with the aforementioned dimensions, it is sufficient to consider only a few image dipoles. By an estimation of the behavior of the potential in the infinite cylinder, it can be proved that the other image dipoles make only a negligible contribution to the sum.

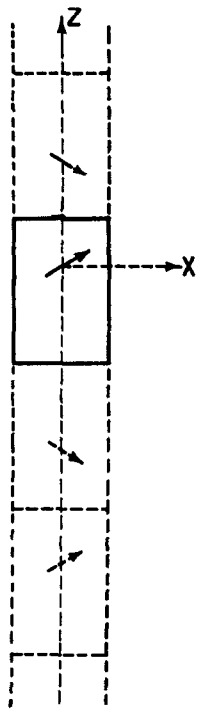

Fig. 14.—Illustration of the method of electrical images. The full lines indicate the intersection of the cylinder with a plane through the axis. The arrow indicates the dipole. The dotted lines indicate the electrical images, the dotted arrows the images of the heart vector.

The same method of electrical images has been used to calculate the field of a dipole between two parallel planes. In that case, we must calculate the sum of the fields in free space of a series of dipoles.

REFERENCES

1. Einthoven, W., Fahr, G., and de Waart, A.: Ueber die Richtung und manifeste Grösse der Potentialschwankungen in menschlichen Herzen und über den Einfluss des Herzlage auf die Form des Elektrokardiogramms, Pflügers Arch. **150**:275, 1913.
2. Burger, H. C., and van Milaan, J. B.: Heart Vector and Leads, Brit. Heart J. **8**:157, 1946.
3. Burger, H. C., and van Milaan, J. B.: Heart Vector and Leads II, Brit. Heart J. **9**:154, 1947.
4. Burger, H. C., and van Milaan, J. B.: Heart Vector and Leads III, Geometrical Representation, Brit. Heart J. **10**:229, 1948.
5. Wilson, F. N., and Bayley, R. N.: The Electric Field of an Eccentric Dipole in a Homogeneous Spherical Conducting Medium, Circulation **1**:84, 1950.
6. Magnus, W., und Oberhettinger, F.: Formeln und Sätze für die speziellen Funktionen der mathematischen Physik, 2. Aufl. Berlin, 1948, Julius Springer.
7. Wilson, F. N., Johnston, F. D., and Kossmann, C. E.: The Substitution of a Tetrahedron for the Einthoven Triangle, AM. HEART J. **33**:594, 1947.